RSC Advances

PAPER

View Article Online
View Journal | View Issue

Open Access Article. Published on 15 October 2018. Downloaded on 12/4/2025 9:14:37 PM.
This article is licensed under a Creative Commons Attribution-NonCommercial 3.0 Unported Licence.

Check for updates

Cite this: *RSC Adv.*, 2018, **8**, 35289

# An unexpected dual-response pH probe based on acridine†

Liang Xu,[a] Xiangzhen Yan[b] and Chunxue Yuan *[a]

Received 31st August 2018
Accepted 10th October 2018

DOI: 10.1039/c8ra07283c

rsc.li/rsc-advances

A new pH fluorescent probe 2,8-bis(acridin-9-ylethynyl)-6*H*,12*H*-5,11-methanodibenzo[*b*,*f*][1,5]diazocine (**TBN**), which has two acridine moieties attached to Tröger's base, is a useful fluorescent probe for monitoring extreme acidic and alkaline pH. **TBN** displays an excellent pH dependent behavior and responds linearly to extreme conditions in the pH ranges of 1.4–3.4 and 12.5–15.0. **TBN** can represent a novel type of fluorescent probe with perfect emission properties in extreme acidic and alkaline conditions by utilizing only one functional group.

## Introduction

pH value plays a significant role in many fields, such as biological processes,[1–3] environmental analysis,[4,5] food production[6,7] and life sciences.[8–10] Moreover, as an important indication of cellular health, abnormal variation of pH may cause some serious diseases. Hence, the sensing and monitoring of pH is of great importance for understanding various pH-dependent physiological and pathological processes.

In recent years, a lot of methods have been applied to detect pH values, such as nuclear magnetic resonance,[11,12] potentiometry,[13,14] absorption spectroscopy[15,16] and fluorescent probes.[17,18] Among them, fluorescent probes have attracted much attention because of their quick response, excellent sensitivity, good selectivity, non-invasive detection and low cost.[19] Till now, the improvements in synthetic methods have directed the development of fluorescent probes with many skeletons, including carbazole,[20–22] BODIPY,[23–25] rhodamine,[26–28] cyanine,[29] *etc.*

Most fluorescence-based pH probes can only exhibit response in weak acid range (pH = 4.5–6.0) or neutral range (pH = 6.8–7.4),[30] but only a few fluorescent probes can work under extreme acidity or extreme alkalinity. Much less attention has been paid to fluorescent probes which are pH-sensitive in the lower pH region (pH < 5) or the higher pH region (pH > 9). Therefore, developing pH fluorescence probes with a wide detection range are becoming increasingly important.[31]

Tröger's base (TB), an old compound first synthesized in 1887, is still attracting wide attention owing to its unique properties as organic functional materials. Our group's recent research suggested that TB can be a good candidate to serve as a good electron-donating moiety in a fluorescent probe.[32] Nowadays, increasing interest has been paid to acridine and its derivatives because of their biological activity and photophysical properties.[33,34] However, the acridine chromophores were normally studied for acidic pH fluorescent probes.[35] In this work, we reported a novel probe 2,8-diethynyl-6*H*,12*H*-5,11-methanodibenzo[*b*,*f*][1,5]diazocine (**TBN**) based on TB and acridine. Surprisingly, compound **TBN** is capable of measuring pH values at extreme conditions, specifically over the two pH ranges: 1.4–3.4 and 12.5–15.0, respectively. To the best of our knowledge, this is the first time that the acridine derivatives were used as an alkaline pH fluorescent probe.

## Experimental section

### Materials and apparatus

All chemicals were purchased from Adamas-beta® and TCI and used without further purification. $^{1}$H NMR and $^{13}$C NMR spectra were recorded on a Bruker AVANCE III MR spectrometer, and the chemical shifts ($\delta$) were expressed in parts per million (ppm) and coupling constants ($J$) in Hertz. Mass spectra were determined with a Thermos Scientific Q Exactive LC-MS/MS system. The photoluminescence (PL) spectra were collected on a Lumina fluorescence spectrophotometer. Ultraviolet-visible (UV-vis) absorption spectra were performed on an Evolution 220 UV-vis spectrophotometer. Deionized water was obtained from a Milli-Q water purification system (Millipore). Thin layer chromatography (TLC) was performed on glass plates coated with 0.20 mm thickness of silica gel. pH values were measured using a PHSJ-3F pH meter (Shanghai LeiCi Device Works, Shanghai, China).

[a]College of Materials Science and Engineering, Tongji University, Caoan Road 4800, Shanghai 201804, P. R. China. E-mail: cxyuan@tongji.edu.cn

[b]Department of Periodontology, School and Hospital of Stomatology, Tongji University, Shanghai Engineering Research Center of Tooth Restoration and Regeneration, Shanghai 200072, P. R. China

† Electronic supplementary information (ESI) available. See DOI: 10.1039/c8ra07283c

Open Access Article. Published on 15 October 2018. Downloaded on 12/4/2025 9:14:37 PM.
This article is licensed under a Creative Commons Attribution-NonCommercial 3.0 Unported Licence.

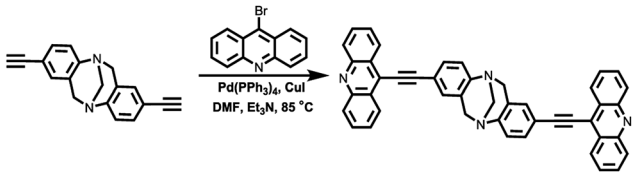


Scheme 1 Synthetic route of TBN.

### Synthesis and characterization of TBN

The synthetic route is depicted in Scheme 1. A mixture of 2,8-diethynyl-6*H*,12*H*-5,11-methanodibenzo[*b*,*f*][1,5]diazocine (130 mg, 0.48 mmol),[36] 9-bromoacridine[37] (272 mg, 1.05 mmol), $Pd(PPh_3)_4$ (56 mg, 0.05 mmol) and CuI (10 mg, 0.05 mmol) were stirred at 85 °C under an atmosphere of $N_2$ for 10 h. Ethyl acetate (10 mL) was added and the solution washed with water (3 × 10 mL) and brine (10 mL). The organic phase was separated, dried and evaporated. The reaction mixture was purified by column chromatography using dichloromethane and petroleum ether (4/1, v/v, $R_f$ = 0.38) as the eluent to give a yellow solid. Yield: 53 mg (21%). $^1$H NMR (400 MHz, 1,1,2,2-tetrachloroethane-$d_2$), $\delta$ (ppm): 4.34 (d, 2H, $J$ = 17.3 Hz), 4.42 (s, 2H), 4.82 (d, 2H, $J$ = 16.8 Hz), 7.29 (d, 2H, $J$ = 8.3 Hz), 7.46 (s, 2H), 7.65 (t, 6H, $J$ = 15.2 Hz), 7.84 (t, 4H, $J$ = 14.8 Hz), 8.30 (d, 4H, $J$ = 6.5 Hz), 8.52 (d, 4H, $J$ = 8.6 Hz). $^{13}$C NMR (101 MHz, 1,1,2,2-tetrachloroethane-$d_2$), $\delta$ (ppm): 58.42, 66.54, 83.57, 99.35, 105.36, 117.52, 120.17, 125.31, 126.21, 126.54, 128.18, 129.41, 130.49, 130.88, 131.27, 147.98, 149.32. HRMS (MALDI-TOF): [$(M + H)^+$] calcd for $C_{45}H_{28}N_4$: 625.2348; found: 625.2291.

### General procedure for spectroscopic measurements

The stock solution of **TBN** (10 μM) was prepared by dissolving **TBN** in a mixed solution (DMSO/$H_2O$, v/v, 2/1). The metal ion solutions were prepared by using KCl, NaCl, $CaCl_2$, $MgCl_2 \cdot 6H_2O$, $CuCl_2 \cdot 2H_2O$, $MnCl_2 \cdot 4H_2O$, $CoCl_2 \cdot 6H_2O$, $NiCl_2 \cdot 6H_2O$, $CdCl_2$, $AlCl_3$, $ZnCl_2$, $CrCl_3 \cdot 6H_2O$, $AgNO_3$, $BaCl_2$, $PbCl_2$, $HgCl_2$. A small amount of HCl or NaOH was added to the solutions to modulate the pH values.

## Results and discussion

### Photophysical properties of probe TBN

In order to gain insight into the photophysical properties of the probe, we investigated the absorption and fluorescent spectra of **TBN** in various solvents with different polarities using 1.0 × $10^{-5}$ mol $L^{-1}$ solutions. As is shown in Fig. 1, **TBN** shows similar absorption spectra and no obvious spectral shift were observed while the emission spectra exhibit quite different spectral lines which are not consistent with the general theoretical predictions of solvent effect.[38] The reasons for the abnormal phenomenon are quite complicated and many factors such as changes in the probe's geometry, solute–solvent interactions and multichromophore aggregation can affect the solvatochromism.[39] The acridine group and the amine on the TB skeleton act as electron acceptor and donor, respectively. This kind of structure enables each wing of **TBN** to form a D–π–A charge motif. Accordingly, the intense fluorescence of **TBN** in solution may owe to the effective intramolecular charge transfer (ICT) through strong push–pull interaction.

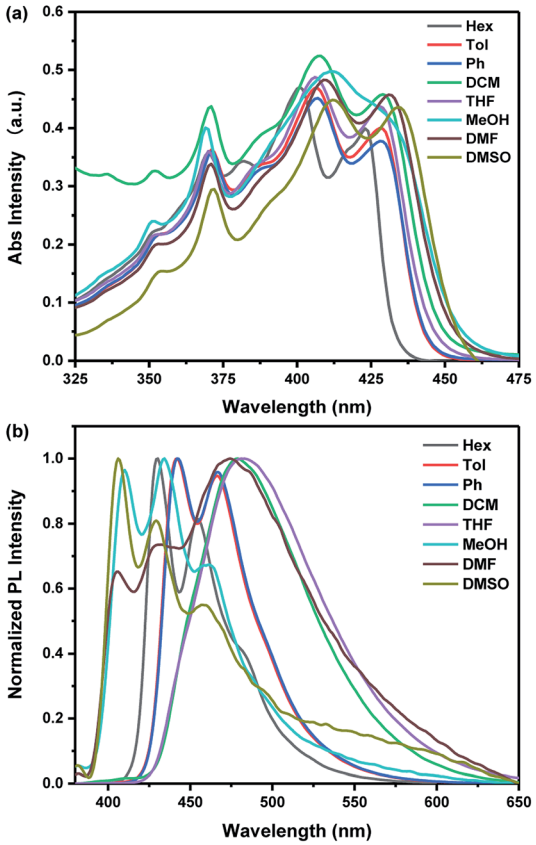


Fig. 1 Normalized (a) UV-vis and (b) PL spectra of TBN in solvents with different polarities.

### UV-vis and fluorescence pH titrations

All samples in UV-vis and fluorescence experiments were performed in aqueous solution (2 : 1, DMSO/$H_2O$, v/v) covering a broad spectrum of pH values ranging from 1.0 to 15.2 (Fig. 2 and 3). To better illustrate this issue, the absorption spectra were divided into two parts: one covers the pH from 15.2 to 7.0,

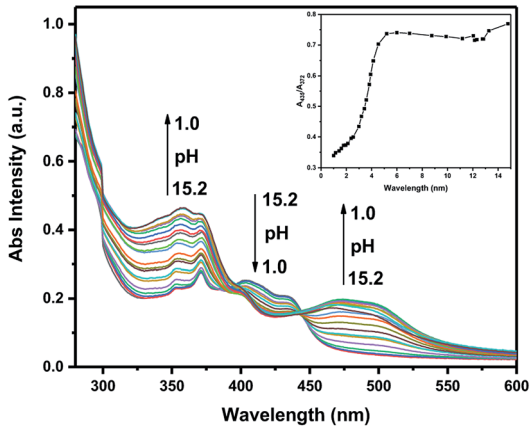


Fig. 2 UV-vis absorption of TBN (10 μM in $H_2O$/DMSO, v/v, 1/2) with different pH values (Inset: plot of ratio of $I_{435}/I_{372}$ as a function of pH).

Open Access Article. Published on 15 October 2018. Downloaded on 12/4/2025 9:14:37 PM.
This article is licensed under a Creative Commons Attribution-NonCommercial 3.0 Unported Licence.

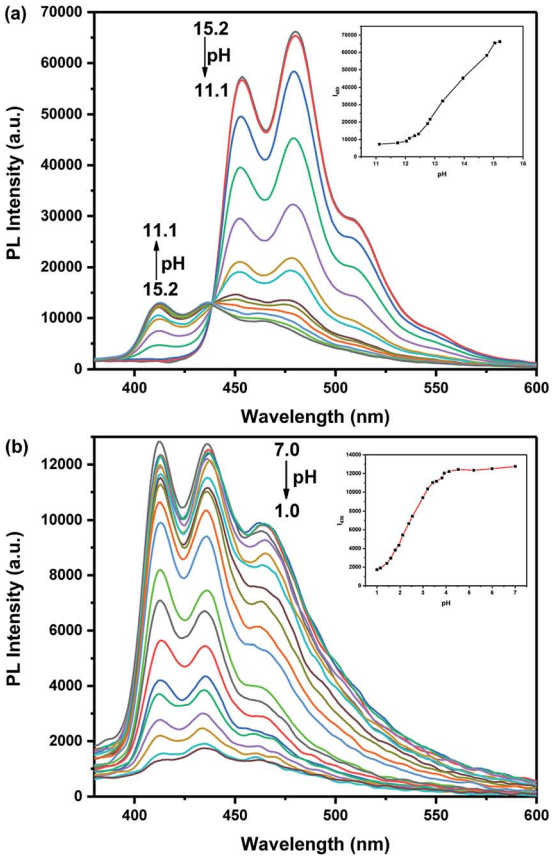


Fig. 3 Fluorescence changes of **TBN** (10 μM) with (a) pH decreased from 15.2 to 11.1. Inset: the variation of fluorescence emission intensity at 480 nm of **TBN** with pH (pH 15.2–11.1), (b) pH decreased from 7.0 to 1.0. Inset: the variation of fluorescence emission intensity at 436 nm of **TBN** with pH (pH 7.0–1.0). Excitation at 320 nm, slit widths were set at 5 nm.

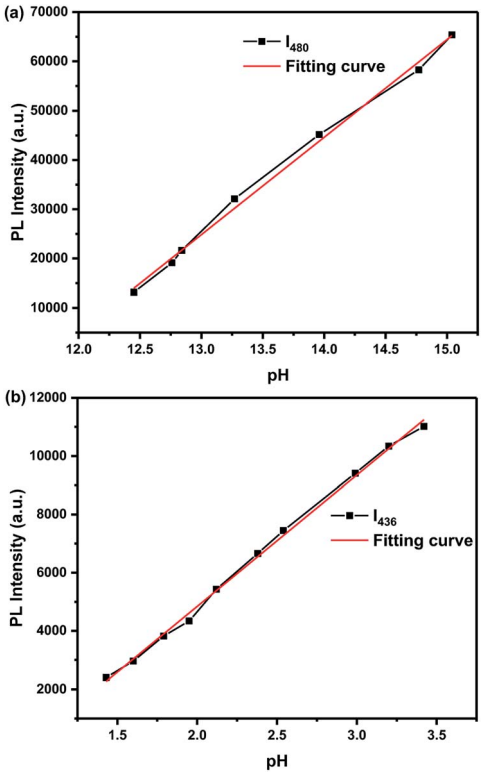


Fig. 4 (a) Fluorescence intensity of probe **TBN** (10 μM, DMSO/$H_2O$, v/v, 2/1) solution as a function of pH from 12.5 to 15.0. $Y = -232351 + 19784X$, $R^2 = 0.9952$. (b) Fluorescence intensity of probe **TBN** (10 μM, DMSO/$H_2O$, v/v, 2/1) solution as a function of pH from 1.4 to 3.4. $Y = -4180 + 4510X$, $R^2 = 0.9975$. $\lambda_{ex} = 320$ nm.

the other covers the pH from 7.0 to 1.0 (Fig. S1†). As the pH is decreased from 15.2 to 7.0, the absorption intensity showed negligible increasing trend. Upon decreasing the pH from 7.0 to 1.0, the original absorption band at 437 nm decreased while the absorbance at around 353 nm, 372 nm and the absorption band between 470 nm and 503 nm gradually increased. In the meantime, the color was almost unchanged in alkaline pH. However, an apparent color change from viridescence to salmon pink was observed upon increasing the acidity which means that the probe has the potential to serve as a "naked-eye" colorimetric indicator for acidic pH.

We found that probe **TBN** is responsive to both acid and alkaline which exceed our expectation. Because the emission spectra showed little change upon decreasing the pH from 11.1 to 7.0 (Fig. S2†), the emission spectra were also divided into two parts: one covers the pH from 15.2 to 11.1, the other covers the pH from 7.0 to 1.0 (Fig. 3). The **TBN** showed three emission peaks at 413 nm, 437 nm and 463 nm when the pH values are below 11.1. With the gradual increase of pH value from 11.1 to 15.2, the fluorescent intensity of **TBN** at 413 nm was reduced. Meanwhile, two peaks and a shoulder appeared at 453 nm, 480 nm and 509 nm. Additionally, the fluorescence changes under acid conditions were also examined. As shown in Fig. 3b, upon decreasing the pH value from 7.0 to 1.0, an evident decrease of the three fluorescent emission peaks was observed with no obvious spectral shift. The fluorescence change was well demonstrated in the fluorescence photos which were shown in the inset of Fig. S2(a).† Good linearity between fluorescent intensity and pH over the range 1.4 to 3.4 and 12.5 to 15.0 was observed by fluorescence titration experiments (Fig. 4). As a result, probe **TBN** can measure extreme pH values over the two pH ranges 1.0–7.0 and 11.1–15.2, respectively.

### Stability, reversibility and selectivity of TBN

In order to determine the impact of time on this detection process, an estimation of the time-dependent fluorescence spectral changes of probe **TBN** at different pH values was carried out. As shown in Fig. S4,† the fluorescence emission responded immediately and the emission intensity remained stable over a long time.

The reversibility is considered as an essential property of a practical fluorescent probe, so the pH value was modulated repeatedly between 1.0 and 7.0, 11.1 and 15.2 five times, and the corresponding emissions were monitored. As shown in Fig. 5, when solutions containing probe **TBN** were changed to low or high pH, no obvious variation in the fluorescence intensity was observed after five cycles. As illustrated in Fig. S3,† the switch of fluorescence signals was also highly reversible between pH 15.2 and 1.0. Besides, the change of solution fluorescence is visible

Open Access Article. Published on 15 October 2018. Downloaded on 12/4/2025 9:14:37 PM.
This article is licensed under a Creative Commons Attribution-NonCommercial 3.0 Unported Licence.

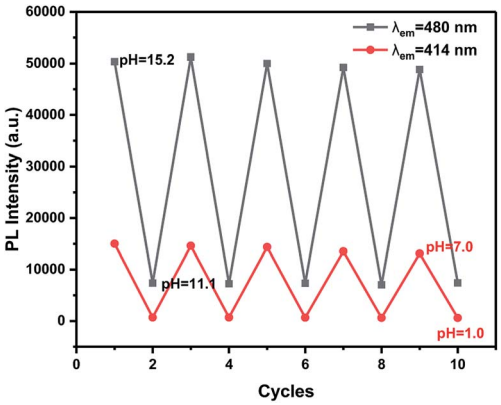


Fig. 5 The pH reversibility of probe TBN.

to the naked eyes. The fast and reversible response to pH fluctuation is necessary for real-time monitoring.

The selectivity of probe **TBN** toward pH was studied by measuring the fluorescence responses to other biologically relevant species including some metal ions and bioactive small molecules at pH 13.8, 7.1, and 1.5, respectively. As shown Fig. 6, no noticeable change was observed in the fluorescence intensity of probe **TBN** with the addition of various interferents, suggesting that the high selectivity of probe **TBN** toward pH.

### Proposed mechanism

In order to get insight into the sensing mechanism of probes **TBN**, $^1$H NMR experiments were carried out under acidic and alkaline conditions in DMSO-$d_6$. As illustrated in Fig. 7, upon addition of hydrochloric acid, the chemical of H1–H4 exhibited an apparent downfield shift. However, the chemical shifts of H8–H10 had little change, which indicated that the protonation

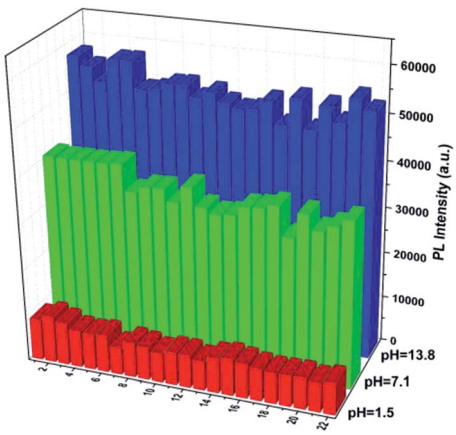


Fig. 6 Fluorescence intensity of 10 μM TBN at different pH in the presence of various species: (1) blank; (2) $K^+$ (150 mM); (3) $Na^+$ (150 mM); (4) $Ca^{2+}$ (0.2 mM); (5) $Mg^{2+}$ (2 mM); (6) $Zn^{2+}$ (0.2 mM); (7) $Cu^{2+}$ (0.2 mM); (8) $Mn^{2+}$ (0.2 mM); (9) $Co^{2+}$ (0.2 mM); (10) $Cr^{3+}$ (0.2 mM); (11) $Cd^{2+}$ (0.2 mM); (12) $Ni^{2+}$ (0.2 mM); (13) $Al^{3+}$ (0.2 mM); (14) $Hg^{2+}$(0.2 mM); (15) histidine (0.2 mM); (16) tyrosine (0.2 mM); (17) arginine (0.2 mM); (18) glutamic acid (0.2 mM); (19) lysine (0.2 mM); (20) threonine (0.2 mM); (21) glycine (0.2 mM); (22) glucose (0.2 mM). Fluorescence intensity at 480 nm at pH 13.8, fluorescence intensity at 436 nm of pH 7.1 and 1.5.

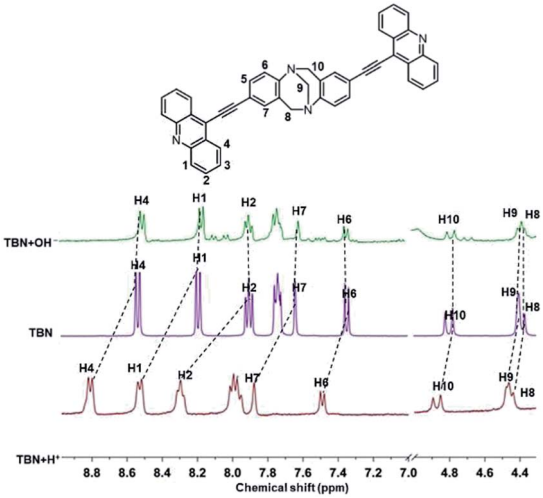


Fig. 7 Partial $^1$H NMR spectrum of TBN, TBN + $H^+$ and TBN + $OH^-$ in DMSO-$d_6$.

occurred at the N atoms in acridine rather than TB skeleton. The downfield chemical shift of these protons was obviously due to $H^+$ binding with N atom of acridine, which enhanced the electron-withdrawing effect, and decreased the electron density of the aromatic ring, leading to the downfield shift of the proton signals. Under the alkaline conditions, all the proton signals of the conjugation system showed little change. To understand this phenomenon better, we introduced 2,8-diethynyl-6*H*,12*H*-5,11-metanodibenzo[*b*,*f*][1,5]diazocine (**TBAN1**) to make a comparison.[40] Interestingly, we found that **TBAN1** showed no response to pH (Fig. S5†). Therefore, it can be concluded that the pH response does not from carbon–carbon triple bonds and the N atoms in the TB skeleton of **TBN**. Moreover, considering the little shift of the alkaline conditions and negligible increasing trend of absorption spectra when the pH decreased from 15.2 to 7.0, it can be regarded as merely a weak interaction between hydroxyl ions and **TBN** molecules. It was reported[41] that acridine emits blue fluorescence only in protic solvents at pH > 11. Weller[42] concluded only the hydrogen-bonded complex between excited acridine and solvent molecules can emit the blue fluorescence. In our case, hydrogen-bonded complex has not been formed in solutions when pH < 11.1, **TBN** molecules in the ground state and protonated **TBN** ions showed purple fluorescence upon irradiation under this condition. In extreme alkaline solutions (pH > 11.1), a rise of the basicity leading to the formation of hydrogen-bonded complex between excited **TBN** dye and solvent molecules which emit intense blue fluorescence upon irradiation.

## Conclusion

In conclusion, we have designed and synthesized an acridine-based fluorescent pH probe **TBN** with excellent selectivity, good stability and high sensitivity. This probe can monitor not only extreme acidic pH but also extreme alkaline pH. The pH titrations demonstrated that probe **TBN** showed an apparent emission decline as the pH decreased from 7.0 to 1.0 and an

Open Access Article. Published on 15 October 2018. Downloaded on 12/4/2025 9:14:37 PM.
This article is licensed under a Creative Commons Attribution-NonCommercial 3.0 Unported Licence.

obvious emission enhancement as the pH increased from 11.1 to 15.2. This probe responds linearly to the extreme acidic range of 1.4–3.4 and to the extreme alkaline range of 12.5–15.0. It is imperative that **TBN** can represent a novel type of fluorescent probe with perfect emission property in the extreme acidic and alkaline conditions by utilizing only one functional group.

## Conflicts of interest

There are no conflicts to declare.

## Acknowledgements

The authors thank the help from Professor Rui Liu in Tongji University on the testing of fluorescence and UV-vis spectra. We gratefully acknowledge the financial support from the state National Natural Science Foundation of China (Grant No. 51403157) and the Fundamental Research Funds for the Central Universities.

## Notes and references

1 W. Niu, L. Fan, M. Nan, Z. Li, D. Lu, M. Wong, S. Shuang and C. Dong, *Anal. Chem.*, 2015, **87**, 2788.
2 N. I. Georgiev, A. I. Said, R. A. Toshkova, R. D. Tzoneva and V. B. Bojinov, *Dyes Pigm.*, 2019, **160**, 28.
3 Y. Ge, A. Liu, J. Dong, G. Duan, X. Cao and F. Li, *Sens. Actuators, B*, 2017, **247**, 46.
4 R. S. Spaulding, M. D. DeGrandpre, J. C. Beck, R. D. Hart, B. Peterson, E. H. Carlo, P. S. Drupp and T. R. Hammar, *Environ. Sci. Technol.*, 2014, **48**, 9573.
5 C. Jeschke, C. Falagán, K. Knöller, M. Schultze and M. Koschorreck, *Environ. Sci. Technol.*, 2013, **47**, 14018.
6 O. Schlüter, B. Rumpold, T. Holzhauser, A. Roth, R. F. Vogel, W. Quasigroch, S. Vogel, V. Heinz, H. Jäger, N. Bandick, S. Kulling, D. Knorr, P. Steinberg and K. Engel, *Mol. Nutr. Food Res.*, 2017, **61**, 1600520.
7 A. Terpou, A. Gialleli, L. Bosnea, M. Kanellaki, A. A. Koutinas and G. R. Castro, *LWT–Food Sci. Technol.*, 2017, **79**, 616.
8 Y. Yue, F. Huo, S. Lee, C. Yin and J. Yoon, *Analyst*, 2017, **142**, 30.
9 J. Chao, K. Song, Y. Zhang, C. Yin, F. Huo, J. Wang and T. Zhang, *Talanta*, 2018, **189**, 150s.
10 J. Chao, K. Song, H. Wang, Z. Li, Y. Zhang, C. Yin, F. Huo, J. Wang and T. Zhang, *RSC Adv.*, 2017, **7**, 964.
11 R. V. Shchepin, D. A. Barskiy, A. M. Coffey, T. Theis, F. Shi, W. S. Warren, B. M. Goodson and E. Y. Chekmenev, *ACS Sens.*, 2016, **1**, 640.
12 G. A. Rothbauer, E. A. Rutter, C. Reuter-Seng, S. Vera, E. J. Billiot, Y. Fang, F. H. Billiot and K. F. Morris, *J. Surfactants Deterg.*, 2018, **21**, 139.
13 L. Truche, E. F. Bazarkina, G. Berger, M. Caumon, G. Bessaque and J. Dubessy, *Geochim. Cosmochim. Acta*, 2016, **177**, 238.
14 Z. Guo, Y. Wang, A. Yang and G. Yang, *Soft Matter*, 2016, **12**, 6669.
15 R. G. Zhang, S. G. Kelsen and J. C. Lamanna, *J. Appl. Physiol.*, 1990, **68**, 1101.
16 J. Han and K. Burgess, *Chem. Rev.*, 2010, **110**, 2709.
17 F. Zhao, L. Zhang, A. Zhu, G. Shi and Y. Tian, *Chem. Commun.*, 2016, **52**, 3717.
18 A. R. Sarkar, C. H. Heo, L. Xu, H. W. Lee, H. Y. Si, J. W. Byun and H. M. Kim, *Chem. Sci.*, 2016, **7**, 766.
19 Y. Ni and J. Wu, *Org. Biomol. Chem.*, 2014, **12**, 3774.
20 L. Fan, S. Gao, Z. Li, W. Niu, W. Zhang, S. Shuang and C. Dong, *Sens. Actuators, B*, 2015, **221**, 1069.
21 F. Miao, G. Song, Y. Sun, Y. Liu, F. Guo, W. Zhang, M. Tian and X. Yu, *Biosens. Bioelectron.*, 2013, **50**, 42.
22 H. Lu, B. Xu, Y. Dong, F. Chen, Y. Li, Z. Li, J. He, H. Li and W. Tian, *Langmuir*, 2010, **26**, 6838.
23 J. Zhang, M. Yang, C. Li, N. Dorh, F. Xie, F. Luo, A. Tiwari and H. Liu, *J. Mater. Chem. B*, 2015, **3**, 2173.
24 J. Qiu, S. Jiang, H. Guo and F. Yang, *Dyes Pigm.*, 2018, **157**, 351.
25 L. Wang, M. Cui, H. Tang and D. Cao, *Anal. Methods*, 2018, **10**, 1633.
26 S. Shen, X. Chen, X. Zhang, J. Miao and B. Zhao, *J. Mater. Chem. B*, 2015, **3**, 919.
27 H. Yu, G. Li, B. Zhang, X. Zhang, Y. Xiao, J. Wang and Y. Song, *Dyes Pigm.*, 2016, **133**, 93.
28 X. Zhao, X. Chen, S. Shen, D. Lia, S. Zhou, Z. Zhou, Y. Xiao, G. Xia, J. Miao and B. Zhao, *RSC Adv.*, 2014, **4**, 50318.
29 Y. Yue, F. Huo, S. Lee, C. Yin, J. Yoon, J. Chao, Y. Zhang and F. Cheng, *Chem.–Eur. J.*, 2017, **22**, 1239.
30 J. Chao, H. Wang, K. Song, Z. Li, Y. Zhang, C. Yin, F. Huo, J. Wang and T. Zhang, *Tetrahedron*, 2016, **72**, 8342.
31 J. Chao, H. Wang, Y. Zhang, Z. Li, Y. Liu, F. Huo, C. Yin and Y. Shi, *Anal. Chim. Acta*, 2017, **975**, 52.
32 C. Yuan, Y. Zhang, H. Xi and X. Tao, *RSC Adv.*, 2017, **7**, 55577.
33 C. Felip-León, O. Martínez-Arroyo, S. Díaz-Oltra, J. F. Miravet, N. Apostolova and F. Galindo, *Bioorg. Med. Chem. Lett.*, 2018, **28**, 869.
34 L. R. Daghigh, M. Pordel and A. Davoodnia, *J. Chem. Res.*, 2014, **38**, 202.
35 S. Chemate, Y. Erande, D. Mohbiya and N. Sekar, *RSC Adv.*, 2016, **6**, 84319.
36 W. Li and T. Michinobu, *Macromol. Chem. Phys.*, 2016, **217**, 863.
37 E. C. Constable, C. E. Housecroft, M. Neuburger and C. X. Schmitt, *Polyhedron*, 2006, **25**, 1844.
38 J. J. Aaront and M. MAAFI, *Spectrochim. Acta*, 1995, **51A**, 603.
39 D. Zhang, Y. Gao, J. Dong, Q. Sun, W. Liu, S. Xue and W. Yang, *Dyes Pigm.*, 2015, **113**, 307.
40 L. Xu, Y. Li, X. Yan and C. Yuan, *Tetrahedron*, 2018, **74**, 4738.
41 E. J. Bowen, N. J. Holder and G. B. Woodger, *J. Phys. Chem.*, 1962, **66**, 2491.
42 A. Weller, *Z. Elektrochem.*, 1957, **61**, 956.